Solving Time-Varying Nonsymmetric Algebraic Riccati Equations With Zeroing Neural Dynamics

Theodore E. Simos, Vasilios N. Katsikis, Spyridon D. Mourtas, and Predrag S. Stanimirović

Abstract—The problem of solving algebraic Riccati equations (AREs) and certain linear matrix equations which arise from the ARE frequently occur in applied and pure mathematics, science, and engineering applications. In this article, by considering the nonsymmetric ARE (NARE) as a general form of ARE, the time-varying NARE (TV-NARE) problem is proposed and investigated. As a particular case of TV-NARE, the time-invariant NARE (TI-NARE) problem is investigated too. Then, by employing the zeroing (or Zhang) neural dynamics (ZND) design, a ZND TV-NARE (ZNDTV-NARE) model and a ZND TI-NARE (ZNDTI-NARE) model are proposed and investigated. Also, by combining the ZNDTV-NARE model with the frozen-time Riccati equation (FTRE) approach to optimal control of linear time-varying (LTV) systems based on the state-dependent Riccati equation (SDRE) process, a hybrid ZND FTRE control (HZND-FTREC) model is developed and investigated. The effectiveness of the proposed dynamical systems is proven in ten numerical experiments, three of which include applications to LTV and nonlinear systems.

Theodore E. Simos is with the Center for Applied Mathematics and Bioinformatics, Gulf University for Science and Technology, West Mishref 32093, Kuwait, also with the Department of Medical Research, China Medical University Hospital, China Medical University, Taichung City 40402, Taiwan, also with the Laboratory of Inter-Disciplinary Problems of Energy Production, Ulyanovsk State Technical University, 432027 Ulyanovsk, Russia, also with the Data Recovery Key Laboratory of Sichun Province, Neijiang Normal University, Neijiang 641100, China, and also with the Section of Mathematics, Department of Civil Engineering, Democritus University of Thrace, 67100 Xanthi, Greece (e-mail: tsimos.conf@gmail.com).

Vasilios N. Katsikis is with the Department of Economics, Division of Mathematics-Informatics and Statistics-Econometrics, National and Kapodistrian University of Athens, 10559 Athens, Greece (e-mail: vaskatsikis@econ.uoa.gr).

Spyridon D. Mourtas is with the Department of Economics, Division of Mathematics-Informatics and Statistics-Econometrics, National and Kapodistrian University of Athens, 10559 Athens, Greece, and also with the Laboratory "Hybrid Methods of Modelling and Optimization in Complex Systems," Siberian Federal University, 660041 Krasnoyarsk, Russia (e-mail: spirosmourtas@gmail.com).

Predrag S. Stanimirović is with the Faculty of Sciences and Mathematics, University of Niš, 18000 Niš, Serbia, and also with the Laboratory "Hybrid Methods of Modelling and Optimization in Complex Systems," Siberian Federal University, 660041 Krasnoyarsk, Russia (e-mail: pecko@pmf.ni.ac.rs).

Color versions of one or more figures in this article are available at https://doi.org/10.1109/TSMC.2023.3284533.

Digital Object Identifier 10.1109/TSMC.2023.3284533

Index Terms—Continuous-time model, dynamical system, nonlinear system, nonsymmetric algebraic Riccati equations (AREs), zeroing neural dynamics.

I. INTRODUCTION

ALGEBRAIC Riccati Equations (AREs) appear commonly in mathematics, science, and engineering. The ARE class includes both nonlinear and linear matrix equations (LMEs) which are specifically of great interest in optimal control, filtering, and estimation problems. The practice has revealed that solving a Riccati equation is a principal topic in optimal control theory (see [1], [2], [3], [4], [5]). The utilization of ARE equations of various types can commonly be found in solving linear multiagent systems [1], in H∞ controller design for wind generation systems [3], in the analysis and synthesis of linear quadratic Gaussian (LQG) control problems [4], [5]. In one or another form, ARE play significant roles in optimal control of multivariable and large-scale systems, estimation, scattering theory, and detection procedures. Moreover, closed-form solutions of Riccati Equations are used to solve some problems, such as numerical precision in direct and iterative algorithms and losing controllability. It is worth noting that other related fields of research are the matrix Ricatti differential equations (MRDEs) (see [6]).

The zeroing (or Zhang) neural dynamics (ZND) method is used to approach the time-varying nonsymmetric ARE (TV-NARE) problem and the time-invariant nonsymmetric ARE (TI-NARE) problem, which is a particular case of TV-NARE, by considering the nonsymmetric ARE (NARE) as a general form of ARE. Because the ZND has already been suggested in the literature as a useful method for solving a wide range of time-variant problems, two models are created by employing the ZND method, namely, the ZND TV-NARE (ZNDTV-NARE) model and the ZND TI-NARE (ZNDTI-NARE) model, which can be solved with exponential convergence performance. Furthermore, the models proposed in [7], [8], [9], [10], and [11] have exponential convergence when the ZND design parameter is adjusted using the ZND method [12], [13], [14], [15] and their speed of convergence can be handled. Compared to traditional numerical algorithms, the ZND method, which is based on recurrent neural networks (RNNs), has several advantages in real-time applications, including high-speed parallel processing, distributed storage, and adaptive self-learning natures. As a result, such an approach is widely regarded as a powerful alternative to online computation and optimization [16], [17], [18], [19].
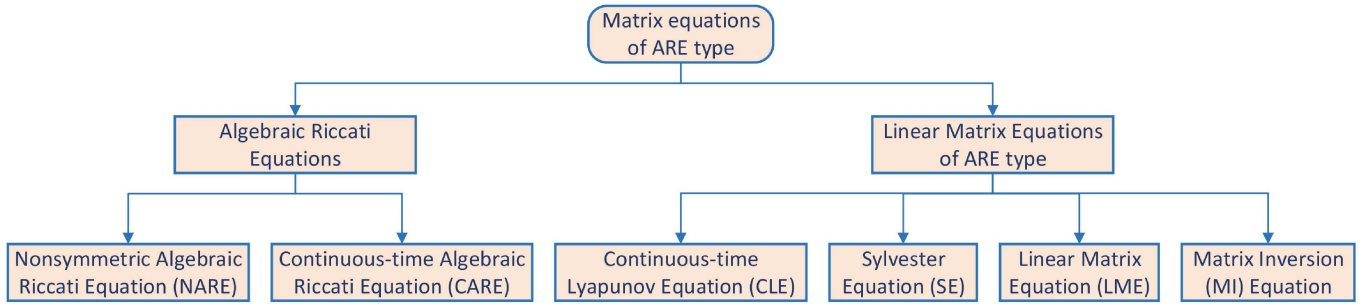
Fig. 1. Diagrammatic representation of the matrix equations explored in this study.

Several papers, including [20] and [21], discuss the ability of such models to handle noise.

A comprehensive overview of ARE-type matrix equations and solutions to some special TV-NARE equations were provided in [21], [22], and [23]. The time-varying ARE problem was approached in [21] through a noise-tolerant ZND model, by a fixed-time ZND model in [22], and by an eigendecomposition-based ZND model in [23]. The symmetric solutions they always offer to the time-varying ARE problem are what these papers have in common. It is crucial to note that AREs with symmetric solutions have square coefficient matrices with certain properties, whereas NAREs are a generic form of AREs whose coefficient matrices are not required to be square with particular properties and whose solutions are not required to be symmetric. Since this study focuses on solving the general TV-NARE problem rather than only the problem of time-varying ARE, it differs significantly from the aforementioned papers.

The tracking control has become one of the most important schemes in past studies [24], [25], [26], [27], [28]. These studies include a position-tracking control strategy using output feedback and an adaptive sliding-mode approach in [24], a hybrid coordinated control method using a backstepping scheme and Hamilton control in [25], a control method using an error-to-actuator-based event-triggered framework [26], and two controllers that combine a backstepping scheme, fuzzy logic system, and finite-time Lyapunov stability theory in [27] and [28]. It is well known that the state-dependent Riccati equation (SDRE) method [3] can be used as a basis for the frozen-time Riccati equation (FTRE) approach to optimal control of linear time-varying (LTV) systems. In this article, by combining the ZNDTV-NARE model and the FTRE, a Hybrid ZND FTRE Control (HZND-FTREC) model is developed and investigated. It is worth noting that the advantages of the HZND-FTREC and ZNDTV-NARE models are the same.

The following summarizes the key contributions of our research in this article.

1) The ZND systems dynamics for solving TV-NARE and TI-NARE problems are proposed. According to our best knowledge, ZND approach for solving NARE has not been used so far.
2) An additional explicit dynamical system is proposed for solving TV-NARE besides the standard ZND.
3) Applying the proposed explicit dynamical system in particular cases, it is possible to generate corresponding

neural dynamics for solving the Sylvester, Lyapunov, and LMEs.
4) Simulation examples are run to validate the proposed model's applicability and effectiveness.
5) Besides the numerical simulations, we present two applications in optimal control of LTV systems and an application in solving nonlinear systems.

The following structure guides the overall organization of sections in this article. Section II contains preliminary information about the ARE and certain LMEs which could be arising from the NARE, including the Sylvester and Lyapunov equations. Section III describes the TV-NARE problem and then defines the corresponding ZNDTV-NARE model. Section IV comprises prominent particular cases of the ZNDTV-NARE design, including the ZNDTI-NARE model. Section V introduces a hybrid TV-NARE model, called HZND-FTREC, which incorporates the FTRE approach to optimal control of the LTV system. Section VI contains ten different examples with different-dimensional input matrices, three of these include LTV and nonlinear system applications. The simulation tests validate the efficacy of the suggested models. Finally, the concluding remarks are presented in Section VII.

II. MATRIX EQUATIONS OF ARE TYPE

This section will provide a comprehensive overview of the matrix equations discussed in this article. These equations are in the form of the pure ARE and certain LMEs derived from the ARE class. A diagrammatic representation of these equations is presented in Fig. 1.

A. Algebraic Riccati Equations

In this section, we introduce the definitions of all the AREs treated in this research.

1) Nonsymmetric Algebraic Riccati Equation: An NARE is a quadratic matrix equation of the form

$$DX + XA - XBX + Q = \mathbf{0} \tag{1}$$

where $A \in \mathbb{R}^{m \times m}$, $B \in \mathbb{R}^{m \times n}$, $D \in \mathbb{R}^{n \times n}$ and $Q \in \mathbb{R}^{n \times m}$ are the block coefficients, $X \in \mathbb{R}^{n \times m}$ is the unknown matrix to be obtained and $\mathbf{0}$ represents a zero $n \times m$ matrix. Note that the term "nonsymmetric" is improperly used to denote that (1) is in its general form without assumption on the symmetry of the matrix coefficients.

2) Continuous-Time Algebraic Riccati Equation: The continuous-time ARE (CARE)

$$A^T X + XA - XBX + Q = \mathbf{0} \tag{2}$$

in which the superscript $()^T$ denotes the transpose operator and all the coefficient matrices belong to $\mathbb{R}^{n \times n}$, is a quadratic matrix equation and plays a central role in the LQR/LQG control, H_2 and H^∞ control, Kalman filtering, and spectral or co-prime factorizations (see [29], [30], [31], [32], [33], [34]). The phrase "continuous-time" in the notation "CARE" is taken from control theory problems in continuous-time, wherefrom (2) emerges. Note that CARE is an NARE where the block coefficients are square (i.e., $m = n$) and $D = A^T$, $B = B^T$, $Q = Q^T$ (see [35]). Moreover, B, Q are symmetric and non-negative definite matrices (i.e., $B = B^T \geq 0$ and $Q = Q^T \geq 0$). Solutions $X \in \mathbb{R}^{n \times n}$ of the CARE (2) can be symmetric or nonsymmetric, with definite or indefinite sign and the solutions set can be either infinite or finite (see [36]).

B. Linear Matrix Equations of ARE Type

In this section, we restate the definitions of all the LMEs arising from the ARE.

1) Continuous-Time Lyapunov Equation: The continuous-time Lyapunov equation (CLE) is a matrix equation given as

$$A^T X + XA + Q = \mathbf{0} \tag{3}$$

where $A \in \mathbb{R}^{n \times n}$, $Q \in \mathbb{R}^{n \times n}$ are the matrix coefficients and $X \in \mathbb{R}^{n \times n}$ is the unknown matrix. Lyapunov methods could be applied successfully in numerous scientific and engineering fields, such as in the analysis of various kinds of nonlinear and linear control systems, in control theory, optimization, signal processing, large space flexible structures, and communications (see [37], [38], [39]). Note that (3) is an appearance of NARE where the block coefficients are square and satisfy $D = A^T$, $B = \mathbf{0}$.

2) Sylvester Equation: The Sylvester equation (SE) is an LME of the form

$$DX + XA + Q = \mathbf{0} \tag{4}$$

where $D \in \mathbb{R}^{n \times n}$, $A \in \mathbb{R}^{m \times m}$, $Q \in \mathbb{R}^{n \times m}$ are the block coefficients and $X \in \mathbb{R}^{n \times m}$ is the unknown matrix to be generated. Equation (4) is an NARE where the block coefficient B satisfies $B = \mathbf{0}$. SE is closely associated with the analysis and synthesis of dynamic systems, such as the design of feedback control systems through pole assignment (see [40], [41]).

C. Linear Matrix Equation

The LME is of the general form

$$DX + Q = \mathbf{0} \tag{5}$$

or

$$XA + Q = \mathbf{0} \tag{6}$$

where $D \in \mathbb{R}^{n \times n}$, $A \in \mathbb{R}^{m \times m}$, $Q \in \mathbb{R}^{n \times m}$ are the block coefficients and $X \in \mathbb{R}^{n \times m}$ is the unknown matrix to be calculated. Note that (5) is an NARE where the block coefficients satisfy $A = \mathbf{0}$ and $B = \mathbf{0}$. Also, (6) is an NARE where $D = \mathbf{0}$ and $B = \mathbf{0}$. LMEs frequently appear in science and engineering fields, such as robotic motion tracking and angle-of-arrival localization [42], [43], [44], [45], [46].

D. Matrix Inversion Equation

The matrix inversion (MI) equation is the LME of the form

$$DX - I_n = \mathbf{0} \tag{7}$$

in which $D \in \mathbb{R}^{n \times n}$ is the block coefficient, I_n denotes the $n \times n$ identity matrix and $X \in \mathbb{R}^{n \times n}$ is unknown approximation of the inverse D^{-1} of D to be obtained. Notice also that (7) is an NARE where the block coefficients are square and $A = \mathbf{0}$, $B = \mathbf{0}$ and $Q = -I_n$. The MI problem is commonly involved in numerous problems of science and engineering, for example, as former steps in optimization, signal processing, electromagnetic systems, and robot inverse kinematics [47], [48], [49].

III. Solving TV-NARE via ZND Method

In this section, both the TI NARE case and the TV NARE case are approached by the ZND method. Note that, based on the analysis provided in Section II, we can observe that it is possible to extract all the remaining equations presented therein from the NARE general form (1). Since 2001, when Zhang and Wang [50] proposed the ZND evolution, this method has been studied and established as a crucial class of RNNs. Furthermore, the ZND evolution has been analyzed theoretically and substantiated comparatively for solving time-varying problems accurately and efficiently. Following the ZND design formula (see [7], [8], [9], [10], [11], [12], [13], [14], [15]) under the linear activation, an appropriately defined error matrix $E(t)$ can dynamically adjusted as a result of the evolution

$$\dot{E}(t) = -\lambda E(t) \tag{8}$$

at which $\dot{()}$ represents the first derivative operator as a function of time t and $\lambda > 0$ represents the ZND design parameter. In addition, the gain parameter λ determines the speed of convergence. It is known that the exponential convergence rate of the ZND dynamics is equal to λ [15]. The larger the value of λ, the higher the convergence speed, and, thus, λ should be set as large as the hardware permits. According to the ZND design formula, $E(t)$ is pushed to converge exponentially to the null matrix.

A. TV-NARE Problem Formulation via ZND Method

Consider the subsequent general type of a TV-NARE

$$D(t)X(t) + X(t)A(t) - X(t)B(t)X(t) + Q(t) = \mathbf{0} \tag{9}$$

where $A(t) \in \mathbb{R}^{m \times m}$, $B(t) \in \mathbb{R}^{m \times n}$, $D(t) \in \mathbb{R}^{n \times n}$, $Q(t) \in \mathbb{R}^{n \times m}$, $X(t) \in \mathbb{R}^{n \times m}$, and $\mathbf{0} \in \mathbb{R}^{n \times m}$. Moreover, $X(t)$ is an unknown matrix of interest.

It is important to mention that the results in [21], [22], and [23] refer to the particular case $D(t) = A^T(t)$ in (9). Our goal is to solve the general TV-NARE problem.

According to (9), the error matrix is equal to

$$E(t) = D(t)X(t) + X(t)A(t) - X(t)B(t)X(t) + Q(t) \quad (10)$$

while its derivative is

$$\dot{E}(t) = \dot{D}(t)X(t) + D(t)\dot{X}(t) + \dot{X}(t)A(t) + X(t)\dot{A}(t)$$
$$- \dot{X}(t)B(t)X(t) - X(t)\dot{B}(t)X(t) - X(t)B(t)\dot{X}(t) + \dot{Q}(t).$$

Consequently, because of (8), the expanded ZND evolution is

$$-\lambda E(t) = \dot{D}(t)X(t) + D(t)\dot{X}(t) + \dot{X}(t)A(t) + X(t)\dot{A}(t)$$
$$- \dot{X}(t)B(t)X(t) - X(t)\dot{B}(t)X(t)$$
$$- X(t)B(t)\dot{X}(t) + \dot{Q}(t)$$

or

$$- \lambda E(t) - \dot{D}(t)X(t) - X(t)\dot{A}(t) + X(t)\dot{B}(t)X(t) - \dot{Q}(t)$$
$$= D(t)\dot{X}(t) + \dot{X}(t)A(t) - \dot{X}(t)B(t)X(t) - X(t)B(t)\dot{X}(t). \quad (11)$$

Note that, to ensure solvability of (11) we cannot include $X(t)$ inside the mass matrix of (11), and to overcome this difficulty, the vectorization procedure and the Kronecker product $\otimes$ are applied on (11). We set as $\mathbf{v}(t)$ the result of vectorization in the left part of (11), so we have

$$\mathbf{v}(t) = \text{vec}\Big(- \lambda E(t) - \dot{D}(t)X(t) - X(t)\dot{A}(t)$$
$$+ X(t)\dot{B}(t)X(t) - \dot{Q}(t)\Big). \quad (12)$$

We repeat the process (i.e., vectorization) in the right part of (11), and we have

$$\text{vec}\Big(D(t)\dot{X}(t) + \dot{X}(t)A(t) - \dot{X}(t)B(t)X(t) - X(t)B(t)\dot{X}(t)\Big)$$
$$= \Big(I_m \otimes D(t) + A(t)^{\text{T}} \otimes I_n - I_m \otimes X(t)B(t)$$
$$- (B(t)X(t))^{\text{T}} \otimes I_n\Big)\text{vec}\big(\dot{X}(t)\big). \quad (13)$$

In addition, by setting

$$M(t) = I_m \otimes D(t) + A(t)^{\text{T}} \otimes I_n - I_m \otimes X(t)B(t)$$
$$- (B(t)X(t))^{\text{T}} \otimes I_n \quad (14)$$

and

$$\dot{\mathbf{x}}(t) = \text{vec}\big(\dot{X}(t)\big)$$

the combination of (13) and (11) results in implicit dynamic behavior shown below

$$\mathbf{v}(t) = M(t)\dot{\mathbf{x}}(t) \quad (15)$$

in which $\mathbf{v}(t)$ is defined by (12). The consistency of the linear system (15) is constrained by

$$M(t)M(t)^{\dagger}\mathbf{v}(t) = \mathbf{v}(t)$$

and its general solution in this case is

$$\dot{\mathbf{x}}(t) = M(t)^{\dagger}\mathbf{v}(t) + \Big(I - M^{\dagger}(t)M(t)\Big)\mathbf{y} \quad (16)$$

such that $\mathbf{y}$ is a vector of proper size. The best approximate solution to the dynamics (15) is given by

$$\dot{\mathbf{x}}(t) = M(t)^{\dagger}\mathbf{v}(t) \quad (17)$$

where $()^{\dagger}$ denotes the pseudoinverse operator. If (15) is solvable, (17) is its solution, while in the opposite case, (17) gives the best approximate solution to (15). Note that {(12), (14), (17)} consist of the suggested ZNDTV-NARE model which could be efficiently solved with the use of an ode MATLAB solver.

According to the previous discussion, we may conclude that (11) cannot be implemented in MATLAB, whereas (17) can. We certainly have the cost of calculating the pseudoinverse of $M(t)$. Theorem 1 proves the exponential convergence of the ZNDTV-NARE {(12), (14), (17)} to the theoretical solution (9).

Theorem 1: Let $A(t) \in \mathbb{R}^{m \times m}$, $B(t) \in \mathbb{R}^{m \times n}$, $D(t) \in \mathbb{R}^{n \times n}$, $Q(t) \in \mathbb{R}^{n \times m}$ be differentiable. The ZNDTV-NARE model {(12), (14), (17)} has exponential convergence to the theoretical solution of TV-NARE (9), for any initial value $X(0)$.

Proof: The error matrix equation $E(t)$ is determined as in (10), inline with the ZND architecture, to achieve the solution $X(t)$ of TV-NARE (9). From [50, Theorem], the solution of (11) converges to the exact solution $X^*(t)$ of (9) as $t \to \infty$. In addition, from the derivation process, the conclusion is that (15) is a vectorized form of (11). As a conclusion, $\mathbf{x}(t)$ defined by the dynamics (15) converges to $\mathbf{x}^*(t) = \text{vec}(X^*(t))$ as $t \to \infty$. Since the convergence $\mathbf{x}(t) \to \mathbf{x}^*(t) = \text{vec}(X^*(t))$ is valid for arbitrary $\dot{\mathbf{x}}(t)$ in (16), it is also valid for $\dot{\mathbf{x}}(t)$ in (17). Thus, the proof is finished. ∎

IV. PARTICULAR CASES OF ZNDTV-NARE DESIGN

The applicability of the defined model is illustrated by several covered cases.

A. TI-NARE Problem Formulation via ZND Method

Consider the general type of a TI-NARE

$$DX(t) + X(t)A - X(t)BX(t) + Q = \mathbf{0} \quad (18)$$

wherein $A \in \mathbb{R}^{m \times m}$, $B \in \mathbb{R}^{m \times n}$, $D \in \mathbb{R}^{n \times n}$, $Q \in \mathbb{R}^{n \times m}$, $X(t) \in \mathbb{R}^{n \times m}$, and $\mathbf{0} \in \mathbb{R}^{n \times m}$. In addition, $X(t) \in \mathbb{R}^{n \times m}$ is an unknown matrix.

By setting the error function

$$E(t) = DX(t) + X(t)A - X(t)BX(t) + Q$$

which fulfills

$$\dot{E}(t) = D\dot{X}(t) + \dot{X}(t)A - \dot{X}(t)BX(t) - X(t)B\dot{X}(t)$$

the general evolution (8) initiates

$$- \lambda E(t) = D\dot{X}(t) + \dot{X}(t)A - \dot{X}(t)BX(t) - X(t)B\dot{X}(t). \quad (19)$$

An application of the vectorization rules to (19) gives

$$\text{vec}(-\lambda E(t))$$
$$= \Big(I_m \otimes D + A^{\text{T}} \otimes I_n - (BX(t))^{\text{T}} \otimes I_n - I_m \otimes X(t)B\Big)\text{vec}\big(\dot{X}(t)\big).$$

Furthermore, by setting

$$\mathbf{v}(t) = -\lambda\text{vec}(E(t)), \qquad \dot{\mathbf{x}}(t) = \text{vec}\big(\dot{X}(t)\big) \quad (20)$$

and

$$M(t) = I_m \otimes D + A^{\mathrm{T}} \otimes I_n - (BX(t))^{\mathrm{T}} \otimes I_n - I_m \otimes X(t)B \tag{21}$$

one obtains the system of linear equations of the form (15). One of the solutions of the implicit system (15) is given by the explicit dynamics (17). Note that {(17), (20), (21)} represents the proposed ZNDTI-NARE model which can efficiently be implemented with the use of an ode *MATLAB* solver.

B. ZNDTV-NARE Design for Solving Particular Equations

The choice of $B(t) \equiv \mathbf{0}$ in NARE makes the ZNDTV-NARE design suitable for solving the TV SE. That is, the TV SE is defined using the error matrix

$$E(t) = D(t)X(t) + X(t)A(t) + Q(t)$$

where $A(t) \in \mathbb{R}^{m \times m}, D(t) \in \mathbb{R}^{n \times n}, Q(t) \in \mathbb{R}^{n \times m}, X(t) \in \mathbb{R}^{n \times m}$. Then, the ZNDTV-NARE design becomes the ZND for solving the TV SE

$$-\lambda E(t) - \dot{D}(t)X(t) - X(t)\dot{A}(t) - \dot{Q}(t)$$
$$= D(t)\dot{X}(t) + \dot{X}(t)A(t). \tag{22}$$

In [51], [52], [53], and [54], various finite-time convergent ZND models of type (22) are used to solve the SE and are centered on appropriate nonlinear activation.

Finite-time convergent RNN models based on improving the standard ZND evolution are considered in [55] and [56].

The proposed explicit dynamical system {(12), (14), (17)} can be applied in solving the TV SE in the particular case

$$\dot{\mathbf{x}}(t) = \mathrm{vec}(\dot{X}(t)) = (I_m \otimes D(t) + A(t)^{\mathrm{T}} \otimes I_n)^{\dagger} \mathbf{v}(t) \tag{23}$$

where

$$\mathbf{v}(t) = \mathrm{vec}(-\lambda E(t) - \dot{D}(t)X(t) - X(t)\dot{A}(t) - \dot{Q}(t)).$$

The choice of $B(t) \equiv \mathbf{0}, D(t) \equiv A(t)^{\mathrm{T}}$ in NARE makes the ZNDTV-NARE design suitable for solving the Lyapunov equation.

ZND models for solving the Lyapunov equation based on appropriate nonlinear activation are considered in [57], [58], [59], and [60]. The finite-time convergent RNN model based on improving the standard ZND evolution was considered in [61].

The following particular case of the explicit dynamical system {(12), (14), (17)} can be applied in solving the TV Lyapunov equation:

$$\dot{\mathbf{x}}(t) = (I_m \otimes (A(t))^{\mathrm{T}} + (A(t))^{\mathrm{T}} \otimes I_n)^{\dagger} \mathbf{v}(t) \tag{24}$$

where

$$\mathbf{v}(t) = \mathrm{vec}(-\lambda E(t) - \dot{A}^{\mathrm{T}}(t)X(t) - X(t)\dot{A}(t) - \dot{Q}(t)).$$

It is essential to mention that the evolution (23) [resp., (24)] has not been used so far in solving the Sylvester (resp., Lyapunov) equation. Finally, the LME (5) can be solved using the dynamics

$$\dot{\mathbf{x}}(t) = (I_m \otimes D(t))^{\dagger} \mathbf{v}(t). \tag{25}$$

The dual LME (6) can be solved using the dynamics

$$\dot{\mathbf{x}}(t) = ((A(t))^{\mathrm{T}} \otimes I_n)^{\dagger} \mathbf{v}(t). \tag{26}$$

V. HYBRID TV-NARE MODEL IN FTRE CONTROL

The backward-in-time Riccati equation, which uses advanced dynamics knowledge to calculate feedback gains over the control horizon, is used to manage optimal control of LTV systems (see [62], [63]). The proposed hybrid model has the ability to stabilize LTV systems. It uses the FTRE approach presented in [2], which is motivated by the equivalent SDRE process. The SDRE technique is a systematic and efficient way to design nonlinear feedback controllers for a wide range of nonlinear systems. More precisely, SDRE is employed for nonlinear dynamics $\dot{z}(t) = f(z, u)$ which can be formulated in the pseudo-linear shape $\dot{z}(t) = A(z, u)z + G(z, u)u$, for which the solution of ARE is generated at each time instant t, as $A(z(t), U(t))$ and $G(z(t), U(t))$ being the chosen dynamics and the input matrices, respectively. The FTRE control is associated with the SDRE approach and includes the factorization

$$\dot{z}(t) = f(z(t), U(t)), \quad z(0) = z_0 \tag{27}$$

into the state-dependent style, where $z \in \mathbb{R}^n$ represents the state vector, $u \in \mathbb{R}^m$ represents the input vector, $f : \mathbb{R}^n \to \mathbb{R}^n$ is a function, and $G : \mathbb{R}^n \to \mathbb{R}^{n \times m}$. The linear structure provided by the factorization is as follows:

$$\dot{z}(t) = A(z(t), U(t))z(t) + G(z(t), U(t))U(t)$$
$$z(0) = z_0. \tag{28}$$

Furthermore, in controller design, state-dependent weighting matrices provide versatility.

The task is to obtain a state-feedback control law in the pattern $U(t) = -K(z(t))z(t)$, which minimizes the cost function of infinite-horizon performance [2]

$$J(z_0, u) = \frac{1}{2} \int_0^{\infty} [z^{\mathrm{T}}(t)R_1(z(t))z(t) + u^{\mathrm{T}}(t)R_2(z(t))U(t)]\mathrm{d}t \tag{29}$$

where $R_1(z) \in \mathbb{R}^{n \times n}$ is positive semidefinite, $R_2(z) \in \mathbb{R}^{m \times m}$ is positive definite. The state-feedback control law is defined as

$$U(t) = -K(z(t))z(t)$$
$$= -R_2^{-1}(z(t))G^{\mathrm{T}}(z(t), U(t))X(z(t))z(t) \tag{30}$$

such that $X(z)$ means the solution of the state-dependent ARE

$$A^{\mathrm{T}}(z)X(z) + X(z)A(z) - X(z)G(z)R_2^{-1}(z)G^{\mathrm{T}}(z)X(z) + R_1(z) = \mathbf{0}. \tag{31}$$

The SDRE approach is heuristic because the control law may not always be optimal and may not have been stabilized. As proposed in [2], we adapt the SDRE approach to LTV systems. In the FTRE process, at each moment, we "freeze" the state and input matrices and deal with them as time-invariant matrices. The solution $X(t)$ to the frozen-time ARE can be launched as a solution to

$$A^{\mathrm{T}}(t)X(t) + X(t)A(t) - X(t)G(t)R_2^{-1}(t)G^{\mathrm{T}}(t)X(t) + R_1(t) = \mathbf{0}. \tag{32}$$

The control law is calculated in the same way as the linear quadratic regulator problem

$$U(t) = -R_2^{-1}(t)G^{\mathrm{T}}(t)X(t)z(t). \tag{33}$$

In [64] and [65], it has been shown that the FTRE control inherits the stability properties of the SDRE controller.

By setting $D(t) = A(t)$, $B(t) = G(t)R_2^{-1}(t)G^{\mathrm{T}}(t)$ and $Q(t) = R_1(t)$ in (9), it is observable that (32) can be solved via the ZNDTV-NARE model {(12), (14), (17)}. Considering that the solution $X(t)$ to (32) is identified, the state-feedback control law of (33) can also be found and then (28) is solvable. Thus, (28) is rewritten as

$$\dot{z}(t) = A(t)z(t) + G(t)\left(-R_2^{-1}(t)G^{\mathrm{T}}(t)X(t)z(t)\right)$$

or in the next equivalent form

$$\dot{z}(t) = \left(A(t) - G(t)R_2^{-1}(t)G^{\mathrm{T}}(t)X(t)\right)z(t). \tag{34}$$

The stability of the SDRE method is demonstrated in Theorem 2, which considers the general infinite-horizon nonlinear regulator problem of minimizing (29) concerning the state x and the control w subject to the nonlinear differential constraint (28). Furthermore, keep in mind that $\mathbb{C}^k$ indicates the space of continuous functions with continuous first k derivatives.

Theorem 2: With respect to the state z and the control U, consider the generic infinite-horizon nonlinear regulator problem of minimizing (29) under the nonlinear differential constraint (28). Let us assume, that $A(z)$, $G(z)$, $R_1(z)$, and $R_2(z)$ belong to $\mathbb{C}^k$ and that $A(z)$ is both a stabilizable and detectable parameterization of the nonlinear system. The SDRE method then generates a closed-loop solution that is locally asymptotically stable.

Proof: It is important to keep in mind that (34) provides the closed-loop solution, i.e.,

$$\dot{z} = \left(A(z) - G(z)R_2^{-1}(z)G^{\mathrm{T}}(z)X(z)\right)z$$
$$= A_c(z)z$$

and the Riccati equation theory guarantees that the closed-loop matrix

$$A_c(z) = A(z) - G(z)R_2^{-1}(z)G^{\mathrm{T}}(z)X(z)$$

is stable at every point z. $X(z)$ and $A_c(z)$ are both smooth due to the smoothness assumptions. We expand the matrix $A_c(z)$ into the partial Taylor series expansion about zero

$$\dot{z} \approx A_c(z)z + \psi(z) \cdot \|z\|$$

with $\psi(z)$ of k order and

$$\lim_{\|z\|\to 0} \psi(z) = 0.$$

The linear term, which involves a constant stable coefficient matrix, prevails the higher-order term in a narrow neighborhood around the origin, resulting in local asymptotic stability. ∎

Setting $D(t) = A^{\mathrm{T}}(t)$, $B(t) = G(t)R_2^{-1}(t)G^{\mathrm{T}}(t)$, $Q(t) = R_1(t)$, (32) yields (9). Based on this, (34) can be rewrittenas

$$\dot{z}(t) = \left(A(t) - B(t)X(t)\right)z(t). \tag{35}$$

Thus, the HZND-FTREC model is obtained by combining (15) and (35) as in the following:

$$\begin{bmatrix} \mathbf{v}(t) \\ \left(A(t) - B(t)X(t)\right)z(t) \end{bmatrix} = \begin{bmatrix} M(t) & \mathbf{0} \\ \mathbf{0} & I_m \end{bmatrix} \begin{bmatrix} \dot{\mathbf{x}}(t) \\ \dot{z}(t) \end{bmatrix}. \tag{36}$$

One explicit form of the dynamics (36) is equal to

$$\begin{bmatrix} \dot{\mathbf{x}}(t) \\ \dot{z}(t) \end{bmatrix} = \begin{bmatrix} M(t) & \mathbf{0} \\ \mathbf{0} & I_m \end{bmatrix}^{\dagger} \begin{bmatrix} \mathbf{v}(t) \\ \left(A(t) - B(t)X(t)\right)z(t) \end{bmatrix}. \tag{37}$$

The proposed HZND-FTREC model is (37), which can efficiently be solved with the use of an ode *MATLAB* solver.

The stability of the HZND-FTREC model (37) is demonstrated in Theorem 2, which considers the general infinite-horizon nonlinear regulator problem of minimizing (29) with respect to the state x and the control w under the nonlinear differential restriction (28).

Theorem 3: With respect to the state z and the control U, consider the generic infinite-horizon nonlinear regulator problem of minimizing (29) under the nonlinear differential constraint (28). Let us assume, that $A(z)$, $G(z)$, $R_1(z)$, and $R_2(z)$ belong to $\mathbb{C}^k$ and that $A(z)$ is both a stabilizable and detectable parameterization of the nonlinear system. The HZND-FTREC method then generates a closed-loop solution that is locally asymptotically stable.

Proof: Because the HZND-FTREC model (37) is composed of the ZNDTV-NARE model {(12), (14), (17)} and the SDRE method, it can be deduced from Theorems 1 and 2 that the HZND-FTREC model (37) generates a locally asymptotically stable closed-loop solution. ∎

VI. NUMERICAL EXAMPLES

This section includes ten examples, four of which are shown to verify the efficacy and accuracy of the ZNDTV-NARE {(12), (14), (17)}, and three more are shown to verify the efficacy and accuracy of the ZNDTI-NARE {(20), (21), (17)}. The examples applied to LTV and nonlinear systems are intended to validate the efficacy and accuracy of the evolution (37). As a preliminary to the following examples, it is necessary to identify the parameters and symbols and provide additional details.

1) The time interval for the computation is limited to [0, 10]. That is, $t_0 = 0$ is the initial time and $t_f = 10$ is the final time.
2) $\|\cdot\|_F$ denotes the Frobenius norm of a matrix.
3) We have set $\lambda = 10$ in all numerical examples in this section, with the exception of the numerical example Section VI-A, where $\lambda = 10, 100, 1000$.
4) The solution of {(17), (20), (21)}, the solution of {(12), (14), (17)}, and the solution of (37) are obtained by employing the ode15s *MATLAB* solver.
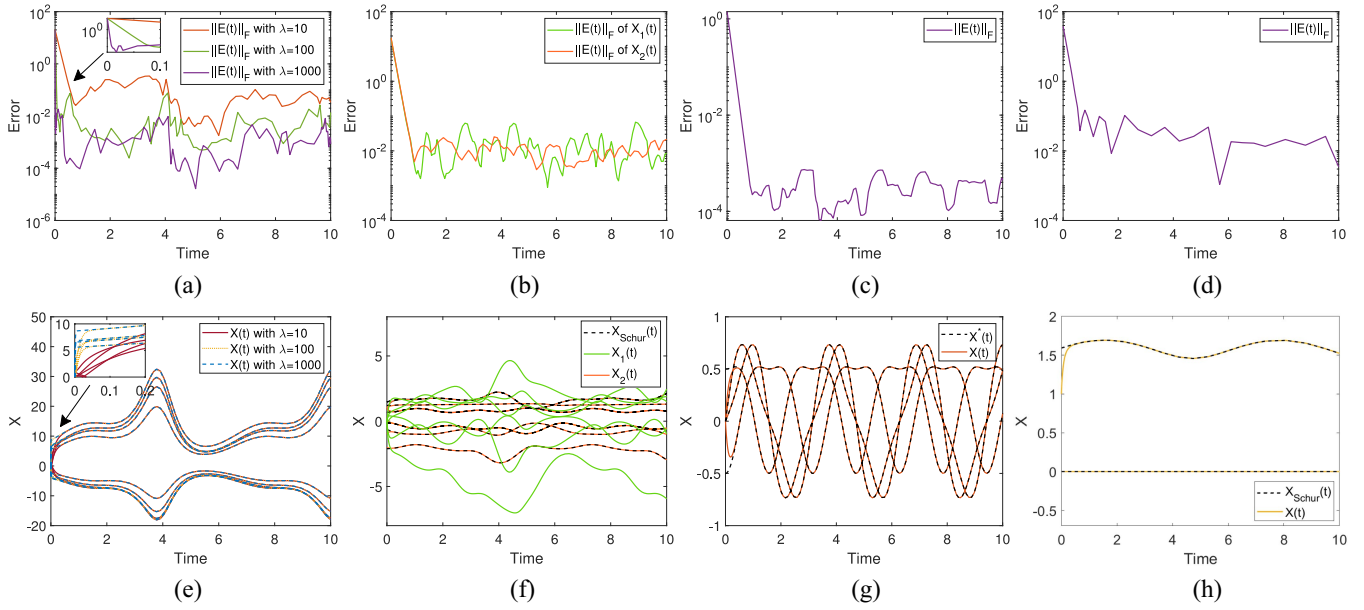
Fig. 2. Performance of ZNDTV-NARE for solving examples Sections VI-A–VI-C and VI-G. (a)–(d) Error $E(t)$ produced by ZNDTV-NARE in examples Sections VI-A–VI-C and VI-G, respectively. (e)–(h) Trajectories of the solution $X(t)$ produced by ZNDTV-NARE in examples Sections VI-A–VI-C and VI-G, respectively.

A. Numerical Example 1

In this example, consider the initial matrices $D(t)$, $A(t)$, $B(t)$, and $Q(t)$ of dimensions 4×4, 2×2, 2×4, and 4×2, respectively, as

$$D(t) = \begin{bmatrix} \sin(t)+1 & \sin(t)+1 & \sin(t)+1 & \sin(2t)+1 \\ \sin(t)+2 & \sin(t)+2 & \sin(t)+2 & \sin(2t)+2 \\ \sin(t)+3 & \sin(t)+3 & \sin(t)+3 & \sin(2t)+3 \\ \sin(t)+4 & \sin(t)+4 & \sin(t)+4 & \sin(2t)+4 \end{bmatrix}$$

$$B(t) = \begin{bmatrix} \sin(t)+1 & \sin(t)+4 & \sin(t)+4 & \sin(t)+4 \\ \sin(t)+4 & \sin(t)+2 & -\sin(t)-5 & \sin(t)+4 \end{bmatrix}$$

$$A(t) = \begin{bmatrix} \cos(t)+3 & \sin(t)+4 \\ \sin(t)+2 & -\sin(t)-7 \end{bmatrix} Q(t) = \begin{bmatrix} \sin(t)+7 & \sin(t)+4 \\ \sin(t)+4 & \sin(t)+6 \\ \sin(t)+1 & \sin(t)+6 \\ \sin(t)+6 & \sin(t)+3 \end{bmatrix}.$$

Setting the initial value of $X(t)$ as $X(0) = \begin{bmatrix} 1 & 0 & 0 & 0 \\ 0 & 1 & 0 & 0 \end{bmatrix}^{\mathrm{T}}$, the results of ZNDTV-NARE are depicted in Fig. 2(a) and (e).

B. Numerical Example 2

Let $A(t)$, $B(t)$, and $Q(t)$ as

$$A(t) = \begin{bmatrix} \sin(t)+2 & \sin(t)+4 & \cos(t)-2 \\ -\sin(t)+4 & \sin(2t)+4 & 3\sin(t)-20 \\ -\cos(2t)-3 & -\sin(t)-2 & -\sin(2t)-5 \end{bmatrix}$$

$$B(t) = \begin{bmatrix} 3\sin(t)+9 & -\sin(t)+5 & \cos(3t)+2 \\ -\sin(t)+5 & \cos(t)+1/2 & \cos(t)+6 \\ \cos(3t)+2 & \cos(t)+6 & \sin(2t)+3/2 \end{bmatrix}$$

$$Q(t) = \begin{bmatrix} 2\sin(t)+10 & \cos(t)+7 & \cos(2t)+3/2 \\ \cos(t)+7 & 2 & -\cos(t)+5 \\ \cos(2t)+3/2 & -\cos(t)+5 & \sin(2t)+4 \end{bmatrix}.$$

Additionally, we set $D(t) = A^{\mathrm{T}}(t)$, transforming in that way the NARE into an ARE. By initializing $X(t)$ with the two

values listed as

$$X_1(0) = \begin{bmatrix} 0 & 0 & 0 \\ 0 & 0 & 0 \\ 0 & 0 & 0 \end{bmatrix} \quad \text{and} \quad X_2(0) = \begin{bmatrix} 1 & 1 & 0 \\ 1 & -1 & 1 \\ 0 & 1 & -2 \end{bmatrix}$$

the results of ZNDTV-NARE are depicted in Fig. 2(b) and (f). Note that Fig. 2(f) also includes the Schur method's suggested solution from [32].

C. Numerical Example 3

The following input matrices $A(t)$ and $Q(t)$ are considered in this example:

$$A(t) = \begin{bmatrix} -1 - 1/2\cos(2t) & 1/2\sin(2t) \\ 1/2\sin(2t) & -1 + 1/2\cos(2t) \end{bmatrix}$$

$$Q(t) = \begin{bmatrix} \sin(2t) & \cos(2t) \\ -\cos(2t) & \sin(2t) \end{bmatrix}.$$

Additionally, we set $B(t) = \mathbf{0}$ and $D(t) = A^{\mathrm{T}}(t)$, converting the NARE to a CLE. By initializing $X(t)$ with $X(0) = \mathbf{0}$, the results of ZNDTV-NARE are depicted in Fig. 2(c) and (g). Note that the theoretical solution of this example is

$$X^{\star}(t) = \begin{bmatrix} \frac{-\sin(2t)(-2+\cos(2t))}{3} & \frac{(1-2\cos(2t))(2+\cos(2t))}{6} \\ \frac{(1+2\cos(2t))(2-\cos(2t))}{6} & \frac{(2+\cos(2t))\sin(2t)}{3} \end{bmatrix}.$$

D. Numerical Example 4

The following constant matrices A, B, and Q of dimensions 2×2 are considered in this example:

$$A = \begin{bmatrix} 4 & 1 \\ -2 & 8 \end{bmatrix}, B = \begin{bmatrix} 7 & 4 \\ 4 & 6 \end{bmatrix}, Q = \begin{bmatrix} 3 & -4 \\ -4 & 5 \end{bmatrix}.$$

Moreover, we convert the NARE to an ARE by using $D(t) = A^{\mathrm{T}}(t)$. Setting

$$X_1(0) = \begin{bmatrix} 2 & -2 \\ -2 & 4 \end{bmatrix}, X_2(0) = \begin{bmatrix} 0 & 0 \\ 0 & 0 \end{bmatrix}, \text{ and } X_3(0) = \begin{bmatrix} 1 & 1 \\ 1 & 1 \end{bmatrix}$$
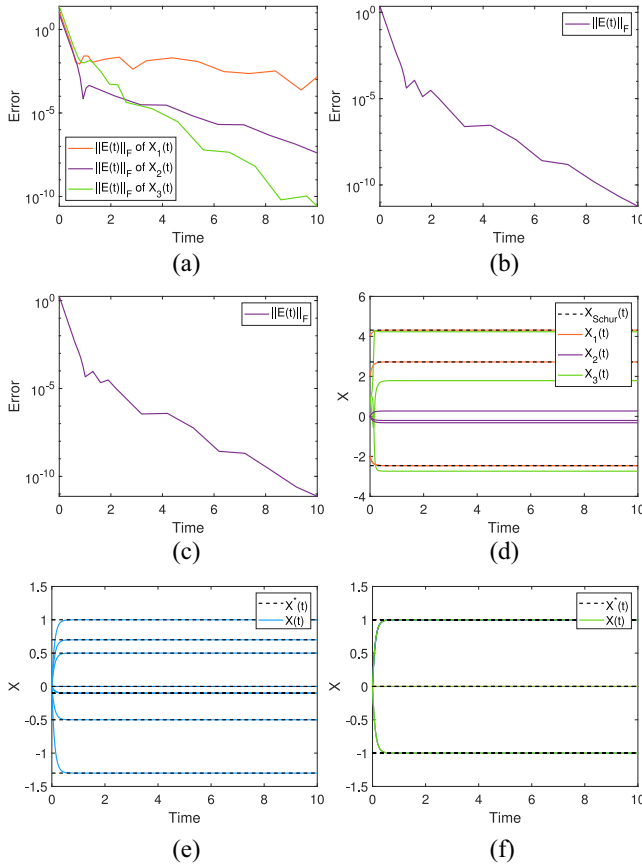
Fig. 3. Performance of ZNDTI-NARE for solving examples Section VI-D–VI-F. (a)–(c) Error $E(t)$ generated by ZNDTI-NARE in examples Section VI-D–VI-F, respectively. (d)–(f) Trajectories of the solution $X(t)$ generated by ZNDTI-NARE in examples Section VI-D–VI-F, respectively.

as three initial values of $X(t)$, the results of ZNDTI-NARE are depicted in Fig. 3(a) and (d). Note that Fig. 3(d) also includes the Schur method's suggested solution from [32].

E. Numerical Example 5

In this example the following matrices D, A, and Q of dimensions 4×4, 2×2, 2×4, and 4×2, respectively, are given as input

$$D = \begin{bmatrix} 1 & 1 & 1 & 1 \\ 1 & 1 & 1 & 1 \\ 0 & 0 & 1 & 0 \\ 0 & 0 & 0 & 1 \end{bmatrix}, \quad A = \begin{bmatrix} 0 & -1 \\ 1 & 0 \end{bmatrix}, \quad Q = \begin{bmatrix} -1 & 0 \\ 1 & 0 \\ 0 & -1 \\ -1 & 1 \end{bmatrix}.$$

Additionally, we convert the NARE to a SE by setting $B = \mathbf{0}$. Setting the initial value of $X(t)$ as $X(0) = \mathbf{0}$, the results of ZNDTI-NARE $\{(17), (20), (21)\}$ are depicted in Fig. 3(b) and (e). Note that the theoretical solution in this example is

$$X^\star(t) = \begin{bmatrix} 0.7 & -1.3 & 0.5 & 0 \\ -0.1 & -0.1 & -0.5 & 1 \end{bmatrix}^{\mathrm{T}}.$$

F. Numerical Example 6

In this example, the input matrices D and Q are given as

$$D = \begin{bmatrix} 1 & 0 & 1 \\ 1 & 1 & 0 \\ 1 & 1 & 1 \end{bmatrix}, \quad Q = \begin{bmatrix} -1 & 0 & 0 \\ 0 & -1 & 0 \\ 0 & 0 & -1 \end{bmatrix}.$$

Additionally, we set $A = B = \mathbf{0}$, so converting the NARE to an MIE. By setting $X(0) = \mathbf{0}$, as the initial value of $X(t)$, the obtained results of ZNDTI-NARE are depicted in Fig. 3(c) and (f). Note that the theoretical solution of this example is

$$X^\star(t) = \begin{bmatrix} 1 & 1 & -1 \\ -1 & 0 & 1 \\ 0 & -1 & 1 \end{bmatrix}.$$

G. Example on Larger Dimensions

The following n-dimensional input matrices are used in this example: $D(t) = (4 + \sin(t))I_n$, $B(t) = (7 + \sin(t))I_n$, $Q(t) = (5 + \sin(t))I_n$. Furthermore, we use $D(t) = A^{\mathrm{T}}(t)$, thus converting the NARE to an ARE. Starting from the initial state of $X(0) = I_n$ and for $n = 50$, the results of ZNDTV-NARE are depicted in Fig. 2(b) and (f). Note that Fig. 2(f) also includes the Schur method's suggested solution from [32].

H. Application to LTV

The Mathieu equation [66] is a linear differential equation with variable (periodic) coefficients and typically occurs in two different ways in solving nonlinear vibration problems. One way is in systems where periodic forcing occurs, and the other is in stability studies of periodic motions in autonomous nonlinear systems. By considering the Mathieu equation

$$\ddot{q}(t) + (\zeta + \theta \cos(\omega t))q(t) = gU(t) \tag{38}$$

and by defining the state vector $z(t) = \begin{bmatrix} q(t) \\ \dot{q}(t) \end{bmatrix}$, the dynamics (38) can be rewritten in state-dependent coefficient form with

$$A(t) = \begin{bmatrix} 0 & 1 \\ (\zeta + \theta \cos(\omega t)) & 0 \end{bmatrix}, \quad G(t) = \begin{bmatrix} 0 \\ g \end{bmatrix}.$$

The parameter values are $\zeta = 1$, $\theta = 1$, $\omega = 1$, $g = 1$, and by letting $R_1 = I_2$, $R_2 = 0.001$ and $R_2 = 1$, we set the initial value of $X(t)$ as $X(0) = \text{ones}(2)$ and apply (37). Furthermore, $z(t)$ has two sets of initial conditions (ICs), denoted as IC1 and IC2. The IC1 corresponds to $z(0) = [3, 0]^{\mathrm{T}}$, and IC2 corresponds to $z(0) = [-5, 1]^{\mathrm{T}}$. Note that the goal should be to drive the states to the equilibrium $[0, 0]^{\mathrm{T}}$ and, hence, to stabilize (38). By applying (37) and the FTRE and FPRE controls [2], the results of phase portraits of the closed-loop responses, for two values of IC, are displayed in Fig. 4(b) for $R_2 = 0.001$, and in Fig. 4(d) for $R_2 = 1$.

I. Applications to Nonlinear Systems

A nonconservative oscillator with nonlinear damping that has been successfully applied in several fields, such as biomedical engineering, power system, control, combustion process, robotics, etc., is the Van der Pol oscillator [67]. As a consequence, Van der Pol oscillator control has considerable practical significance. In this application, we consider the FPRE stabilization of the Van der Pol oscillator

$$\ddot{q}(t) - \mu\left(1 - q^2(t)\right)\dot{q}(t) + q(t) = gU(t) \tag{39}$$
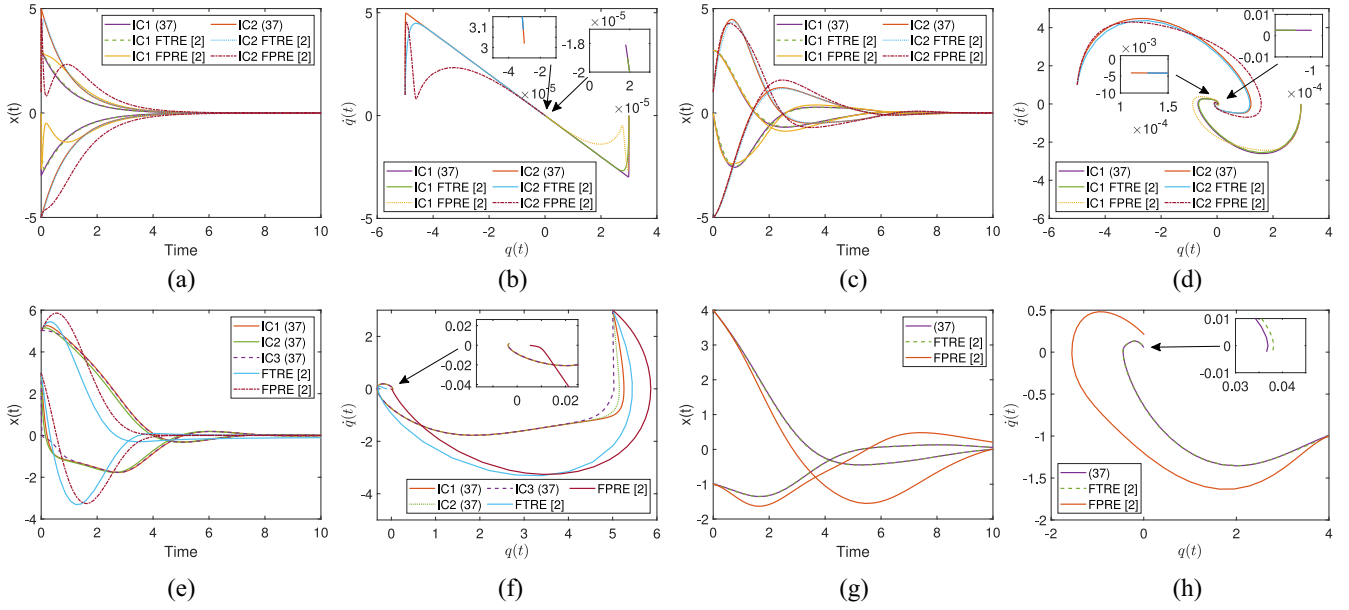
Fig. 4. Results of HZND-FTREC (37), FTRE, and FPRE [2] for solving the Mathieu Equation and stabilizing the Van der Pol oscillator and a spring–mass system. (a) and (b) Mathieu Equation's closed-loop outputs and associated phase portraits with $R_2 = 0.001$. (c) and (d) Mathieu Equation's closed-loop outputs and associated phase portraits with $R_2 = 1$. (e) and (f) Van der Pol oscillator's closed-loop outputs and associated phase portraits. (g) and (h) Closed-loop outputs and associated phase portraits for the mass joined to a wall through a spring.

where $\mu > 0$ and g are real numbers. Defining the state vector $z(t) = \begin{bmatrix} q(t) \\ \dot{q}(t) \end{bmatrix}$, (39) can be written in state-dependent coefficient form with $A(t) = \begin{bmatrix} 0 & 1 \\ 1 & \mu(1 - q^2(t)) \end{bmatrix}$, $G(t) = \begin{bmatrix} 0 \\ g \end{bmatrix}$.

In this application, we use the parameter values $\mu = 0.25$, $g = 1$, and let $z(0) = [5, 3]^T$, $R_1 = I_2$, and $R_2 = 1$. Furthermore, we consider three options of IC, namely, IC1, IC2, and IC3, where we have set as initial values of $X(t)$, $X_1(0) = \text{zeros}(2)$, $X_2(0) = 10I_2$, and $X_3(0) = 100I_2$, respectively. By applying (37) and the FTRE and FPRE controls [2], the generated results of phase portraits of the closed-loop responses for three sets of IC are displayed in Fig. 4(f).

J. Application to Specific Scenario

This application considers a mass that is connected to a wall by a spring with variable stiffness $k(t)$. The open-loop system is described by

$$z(t) = \begin{bmatrix} q(t) \\ \dot{q}(t) \end{bmatrix}, \ A(t) = \begin{bmatrix} 0 & 1 \\ -\frac{k(t)}{m} & 0 \end{bmatrix}, \ G(t) = \begin{bmatrix} 0 \\ \frac{1}{m} \end{bmatrix}$$

where $q(t)$ signifies the position, $k(t)$ signifies the stiffness, which varies over time and can be positive or negative, and $\dot{q}(t)$ signifies the mass's velocity. Let $k(t) = \sin(t)$, $m = 4$, $R_1(t) = I_2$, and $R_2(t) = 1$, we initialize $X(t)$ and $z(t)$ with $X(0) = \text{ones}(2)$ and $z(0) = [4, -1]^T$. By applying (37) and the FTRE and FPRE controls [2], the generated results of phase portraits of the closed-loop responses are displayed in Fig. 4(h).

K. Analysis of Experimental Results

In this section, the presented experimental results for the ZNDTV-NARE, ZNDTI-NARE, and HZND-FTREC

are commented on and analyzed. In numerical examples Section VI-A–VI-C, we notice that the error $\|E(t)\|_F = \|D(t)X(t) + X(t)A(t) - X(t)B(t)X(t) + Q(t)\|_F$, rapidly converges to zero in Fig. 2(a)–(d). That is, ZNDTV-NARE (9) is convergent. Particularly, Fig. 2(a) includes three errors produced from three different design parameter values, i.e., $\lambda = 10, 100, 1000$. The graphs in this figure demonstrate that the model produces a lower overall error with a faster convergence as the value of the parameter λ increases. Fig. 2(b) includes two errors produced from two initial values of $X(t)$ in Example Section VI-B. The graphs in this figure show that the initial values of $X(t)$ have no impact on the model's overall error or speed of the convergence. In Fig. 2(e) and (f) trajectories of the solution $X(t)$ produced by ZNDTV-NARE are presented, wherefrom it is observable that $X(t)$ rapidly converges to the exact solution. Particularly, Fig. 2(e) includes three solutions produced from three different design parameter values, i.e., $\lambda = 10, 100, 1000$. The graphs in this figure show that as the parameter λ increases, the model generates the same solution but with a faster convergence. Fig. 2(f) includes trajectories of two solutions produced from two initial values of $X(t)$ in Example Section VI-B as well as the solution provided by the Schur method originated in [32]. The graphs in Fig. 2(f) show the influence of the initial values for $X(t)$ on the model's solution. It is clear that the ZND model generates various solutions $X_1(t)$ and $X_2(t)$ depending on the initial values of $X(t)$. Fig. 2(g) and (h) include the theoretical and the Schur's method solution, respectively.

In numerical examples Section VI-D-VI-F, we observe that the error $\|E(t)\|_F = \|DX(t) + X(t)A - X(t)BX(t) + Q\|_F$, is rapidly convergent to 0 in Fig. 3(a)–(c). That is, ZNDTI-NARE (18) is solved. Fig. 3(a) includes three errors produced from three initial values in Example Section VI-D. The solution $X(t)$ produced by ZNDTI-NARE is presented in
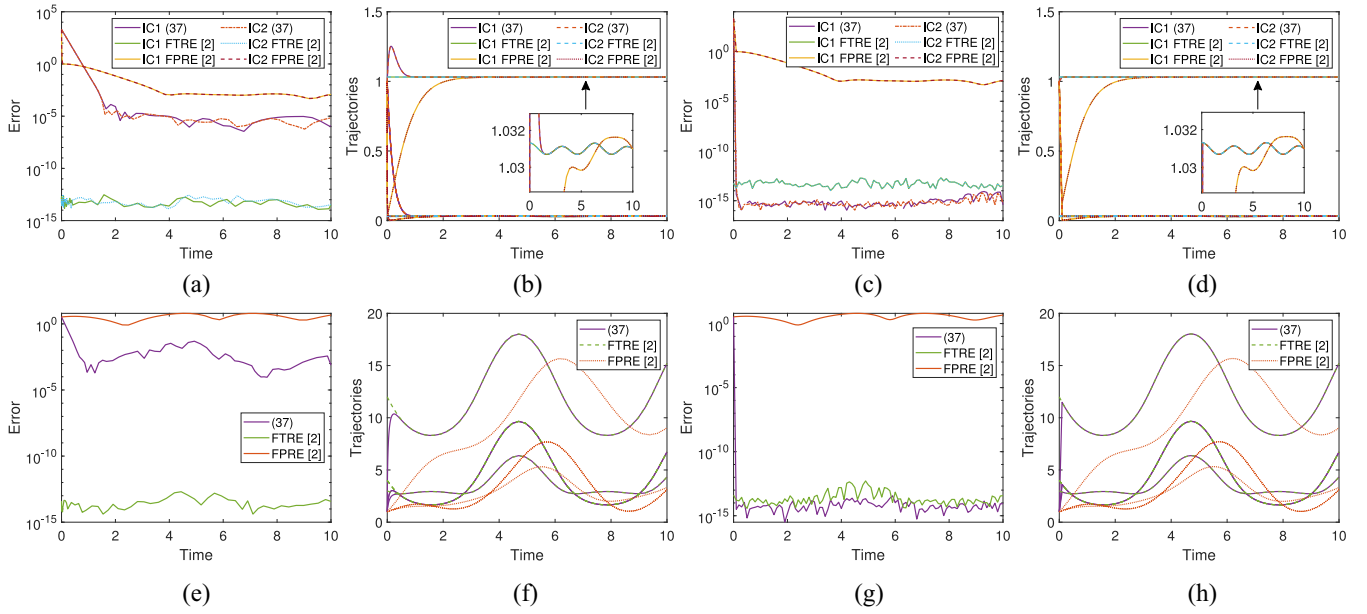
Fig. 5. Results of HZND-FTREC (37), FTRE, and FPRE [2] for solving the Mathieu Equation with $R_2 = 0.001$ and stabilizing a spring–mass system under various settings of ode15s *MATLAB* solver. (a) and (b) Mathieu Equation's ARE error under default settings of ode15s *MATLAB* solver. (c) and (d) Mathieu Equation's ARE trajectories under custom settings of ode15s *MATLAB* solver. (e) and (f) Spring–mass system's ARE error under default settings of ode15s *MATLAB* solver. (g) and (h) Spring–mass system's ARE trajectories under custom settings of ode15s *MATLAB* solver.

Fig. 3(d)–(f), where we see that $X(t)$ quickly converges to the solution. The graphs in Fig. 3(a) and (d) illustrate the behavior of solutions $X_1(t), X_2(t), X_3(t)$ generated by the initial values of $X(t)$ in example Section VI-D. Fig. 3(a) shows the influence of the initial values on the error matrix $\|E(t)\|_F$ generated by $X_1(t), X_2(t), X_3(t)$. Graphs in Fig. 3(d) show the trajectories of elements in $X_1(t), X_2(t), X_3(t)$. It is clear that the ZND model generates various solutions $X_1(t), X_2(t), X_3(t)$ depending on the initial values. Fig. 3(d) includes three solutions produced for three different initial values of $X(t)$ as well as the solution provided by the Schur method from [32]. Furthermore, Fig. 3(e) and (f) includes graphs of theoretical solutions.

In addition, the following is important to mention about numerical examples Section VI-A–VI-G.
1) The coefficient matrices in Sections VI-B, VI-D, and VI-G converted the NARE to an ARE.
2) The input coefficient matrices in Section VI-C converted the NARE to a CLE.
3) The input coefficient matrices in Section VI-E converted the NARE to an SE.
4) The input coefficient matrices in Section VI-F converted the NARE to an MIE.

In applications Section VI-H–VI-J, the asymptotic stability of the HZND-FTREC (37) is always slightly better than the stability of the FTRE control [2] and significantly better than that of the FPRE control [2]. More precisely, in application to LTV Section VI-H, the Mathieu equation is stabilized for two different ICs of $z(t)$ under two different values in R_2. The closed-loop responses of $z(t)$ and their phase portraits are displayed in Fig. 4(a) and (c) and (b) and (d), respectively, where we observe that HZND-FTREC of (37) provides faster stabilization than the FTRE and FPRE controls, even for large values of R_2. In application to nonlinear systems Section VI-I, the Van der Pol oscillator is stabilized for three different initial

values of $X(t)$. The closed-loop responses of $z(t)$ and their phase portraits are displayed in Fig. 4(e) and (f), where we observe that HZND-FTREC of (37) provides, slightly, more stable asymptotic behavior than the FTRE and FPRE controls. In application to specific scenario Section VI-J, a mass connected to a wall by a spring with variable stiffness $k(t)$ is stabilized. In Fig. 4(g) and (h), the closed-loop responses of $z(t)$ and their phase portraits are displayed, where we observe that HZND-FTREC of (37) provides, slightly, more stable asymptotic behavior than the FTRE and FPRE controls.

To further validate the performance of the HZND-FTREC model (37) and demonstrate the distinction between the HZND-FTREC, FTRE, and FPRE controls, the ARE error $\|AX(t) + X(t)A - X(t)BX(t) + Q\|_F$ of the applications Section VI-H and VI-J is measured under various settings of ode15s *MATLAB* solver. It is important to note that all numerical examples and applications in this section have used the default settings of ode15s *MATLAB* solver calculating with double precision ($eps = 2.22 \cdot 10^{-16}$). Therefore, the minimum value for most error measurements in this section is of the order 10^{-5}. For the custom settings used in the results of Fig. 5, we set the relative tolerance and the absolute tolerance of ode15s to 10^{-15}, while the design parameter was set to $\lambda = 10^4$. Particularly, Fig. 5(a) and (e) shows the ARE errors of Mathieu Equation with $R_2 = 0.001$ and spring–mass system, respectively, under the default settings of ode15s and the design parameter $\lambda = 10$. In these figures, we observe that the FTRE that uses the Schur method's suggested solution has the best accuracy and the FPRE has the worst accuracy. When using the custom settings, the ARE errors of Mathieu Equation with $R_2 = 0.001$ and spring–mass system are presented in Fig. 5(c) and (g). In these figures, we note that the HZND-FTREC has the best accuracy, while the performance of FTRE and FPRE is unaffected by the

changes in the settings of the `ode15s`. This conclusion is further supported by a comparison between the ARE trajectories shown in Fig. 5(b) and (f) and those shown in Fig. 5(d) and (h), respectively. While the ARE trajectories generated by FTRE and FPRE are unaffected by the changes in the `ode15s` settings, we observe in these figures that the ARE trajectories generated by HZND-FTREC converge faster to the ARE trajectories generated by FTRE. We also observe that FPRE generates a different and less accurate ARE solution than FTRE in both applications. The HZND-FTREC generates the same ARE solution as the FTRE, and under the `ode15s` custom settings, the HZND-FTREC solution is more accurate than FTRE's.

Consequently, we can say that the TV-NARE problem (9), the TI-NARE problem (18), and HZND-FTREC problem (37) can be successfully solved by the ZNDTV-NARE, ZNDTI-NARE, and HZND-FTREC, respectively, while the HZND-FTREC is a more advanced version of the FTRE and is more effective than both the FTRE and FPRE.

VII. Conclusion

This article examines the TV-NARE problem in detail. The ZND approach, in conjunction with the definition of a convenient error matrix for addressing the TV-NARE problem, led to the development of the suggested ZNDTV-NARE model. Several particular cases of ZNDTV-NARE design are derived, including the ZNDTI-NARE model, and models for solving Sylvester and Lyapunov equation. Furthermore, a hybrid TV-NARE model, called HZND-FTREC, is introduced to incorporate the FTRE approach to optimal control of the LTV system. Computer simulation further showed that the proposed models successfully solved ten examples, three of which included applications to LTV and nonlinear systems. In that manner, the efficacy of the proposed flows for solving the TV-NARE, TI-NARE, and optimal control of LTV systems has thus been demonstrated. The finding reached is that the ZNDTV-NARE, ZNDTI-NARE, and HZND-FTREC models are helpful and efficient in solving the TV-NARE, TI-NARE, and optimal control of LTV systems, respectively. It is worth mentioning that the ZNDTV-NARE model's ability to provide several solutions for various initial values without allowing the user to specify a particular solution as the target is a disadvantage.

Some areas of future research can be pointed out.

1) The ZNDTV-NARE and HZND-FTREC streams can be investigated using a nonlinear activation function. Nonlinear ZNDTV-NARE and HZND-FTREC flows with terminal convergence could be studied in this direction. This approach will be a generalization of finite-time convergent nonlinearly activated dynamical systems for calculating the time-varying matrix pseudoinverse [14], as well as for solving the time-varying SE [42], [43], [51], [58].

2) It is helpful to extend recently proposed finite-time convergent neural flows for solving time-varying linear complex matrix equations [7] or the time-varying Sylvester matrix equation [55] into more general finite-time convergent ZNDTV-NARE and HZND-FTREC evolutions.

3) The open area of research in machine control that is related to fuzzy logic (see [27], [28], [68]) could be paired with the ZND design. This research will lead to the creation of novel ZND designs for tracking control of nonlinear systems.

4) Because all types of noise have a significant impact on the accuracy of the proposed ZND approaches, the proposed ZNDTV-NARE, ZNDTI-NARE, and HZND-FTREC models suffer from noise insensitivity. Future research can be directed at expanding derived models into integration-enhanced and noise-tolerant ZND dynamical systems.

5) As analyzed in the introduction, heterogeneous ARE variants are involved in solutions to numerous continuous time or discrete time problems. Each of these applications provides the possibility of applying the proposed models or their discretization.

6) Note that convergence occurs faster for greater values of λ. For further noteworthy characteristics and variations of the ZND's design parameter λ see [15], [69].

References

[1] X. Dong and G. Hu, "Time-varying formation tracking for linear multiagent systems with multiple leaders," *IEEE Trans. Autom. Control*, vol. 62, no. 7, pp. 3658–3664, Jul. 2017.

[2] A. Prach, O. Tekinalp, and D. S. Bernstein, "A numerical comparison of frozen-time and forward-propagating Riccati equations for stabilization of periodically time-varying systems," in *Proc. Amer. Control Conf.*, 2014, pp. 5633–5638.

[3] B. Qin et al., "Robust H_∞ control of doubly fed wind generator via state-dependent Riccati equation technique," *IEEE Trans. Power Syst.*, vol. 34, no. 3, pp. 2390–2400, May 2019.

[4] T. E. Duncan, L. Guo, and B. Pasik-Duncan, "Adaptive continuous-time linear quadratic Gaussian control," *IEEE Trans. Autom. Control*, vol. 44, no. 9, pp. 1653–1662, Sep. 1999.

[5] A. Kawamoto and T. Katayama, "The dissipation inequality and generalized algebraic Riccati equation for linear quadratic control problem of descriptor system," *IFAC Proc. Vol.*, vol. 29, no. 1, pp. 1548–1553, 1996.

[6] R.-C. Li and W. Kahan, "A family of anadromic numerical methods for matrix Riccati differential equations," *Math. Comput.*, vol. 81, pp. 233–265, Jan. 2012.

[7] L. Xiao, "A finite-time convergent neural dynamics for online solution of time-varying linear complex matrix equation," *Neurocomputing*, vol. 167, pp. 254–259, Nov. 2015.

[8] Y. Zhang and C. Yi, *Zhang Neural Networks and Neural-Dynamic Method*. New York, NY, USA: Nova Sci. Publ., Inc., 2011.

[9] L. Xiao, "A nonlinearly-activated neurodynamic model and its finite-time solution to equality-constrained quadratic optimization with nonstationary coefficients," *Appl. Soft Comput.*, vol. 40, pp. 252–259, Mar. 2016.

[10] B. Liao and Y. Zhang, "Different complex ZFs leading to different complex ZNN models for time-varying complex generalized inverse matrices," *IEEE Trans. Neural Netw. Learn. Syst.*, vol. 25, no. 9, pp. 1621–1631, Sep. 2014.

[11] P. S. Stanimirović, S. D. Mourtas, V. N. Katsikis, L. A. Kazakovtsev, and V. N. Krutikov, "Recurrent neural network models based on optimization methods," *Mathematics*, vol. 10, no. 22, p. 4292, 2022.

[12] L. Jin, S. Li, L. Xiao, R. Lu, and B. Liao, "Cooperative motion generation in a distributed network of redundant robot manipulators with noises," *IEEE Trans. Syst., Man, Cybern., Syst.*, vol. 48, no. 10, pp. 1715–1724, Oct. 2018.

[13] Y. Zhang, L. Jin, D. Guo, Y. Yin, and Y. Chou, "Taylor-type 1-step-ahead numerical differentiation rule for first-order derivative approximation and ZNN discretization," *J. Comput. Appl. Math.*, vol. 273, pp. 29–40, Jan. 2015.

[14] B. Liao and Y. Zhang, "From different ZFs to different ZNN models accelerated via Li activation functions to finite-time convergence for time-varying matrix pseudoinversion," *Neurocomputing*, vol. 133, pp. 512–522, Jun. 2014.

[15] V. N. Katsikis, P. S. Stanimirović, S. D. Mourtas, L. Xiao, D. Karabasević, and D. Stanujkić, "Zeroing neural network with fuzzy parameter for computing pseudoinverse of arbitrary matrix," *IEEE Trans. Fuzzy Syst.*, vol. 30, no. 9, pp. 3426–3435, Sep. 2022.

[16] L. Jin, Y. Zhang, S. Li, and Y. Zhang, "Modified ZNN for time-varying quadratic programming with inherent tolerance to noises and its application to kinematic redundancy resolution of robot manipulators," *IEEE Trans. Ind. Electron.*, vol. 63, no. 11, pp. 6978–6988, Nov. 2016.

[17] L. Xiao and B. Liao, "A convergence-accelerated Zhang neural network and its solution application to Lyapunov equation," *Neurocomputing*, vol. 193, pp. 213–218, Jun. 2016.

[18] D. Guo, Z. Nie, and L. Yan, "Novel discrete-time Zhang neural network for time-varying matrix inversion," *IEEE Trans. Syst., Man, Cybern., Syst.*, vol. 47, no. 8, pp. 2301–2310, Aug. 2017.

[19] V. N. Katsikis, S. D. Mourtas, P. S. Stanimirović, and Y. Zhang, "Solving complex-valued time-varying linear matrix equations via QR decomposition with applications to robotic motion tracking and on angle-of-arrival localization," *IEEE Trans. Neural Netw. Learn. Syst.*, vol. 33, no. 8, pp. 3415–3424, Aug. 2022.

[20] T. E. Simos, V. N. Katsikis, S. D. Mourtas, P. S. Stanimirović, and D. Gerontitis, "A higher-order zeroing neural network for pseudoinversion of an arbitrary time-varying matrix with applications to mobile object localization," *Inf. Sci.*, vol. 600, pp. 226–238, Jul. 2022.

[21] H. Jerbi et al., "Towards higher-order zeroing neural network dynamics for solving time-varying algebraic Riccati equations," *Mathematics*, vol. 10, p. 4490, Nov. 2022.

[22] T. E. Simos, V. N. Katsikis, S. D. Mourtas, and P. S. Stanimirović, "Finite-time convergent zeroing neural network for solving time-varying algebraic Riccati equations," *J. Franklin Inst.*, vol. 359, no. 18, pp. 10867–10883, 2022.

[23] T. E. Simos, V. N. Katsikis, S. D. Mourtas, and P. S. Stanimirović, "Unique non-negative definite solution of the time-varying algebraic Riccati equations with applications to stabilization of LTV systems," *Math. Comput. Simul.*, vol. 202, pp. 164–180, Dec. 2022.

[24] A. Safa, R. Y. Abdolmalaki, and H. C. Nejad, "Precise position tracking control with an improved transient performance for a linear piezo-electric ceramic motor," *IEEE Trans. Ind. Electron.*, vol. 66, no. 4, pp. 3008–3018, Apr. 2019.

[25] W. Sun, Y. Wu, and L. Wang, "Trajectory tracking of constrained robotic systems via a hybrid control strategy," *Neurocomputing*, vol. 330, pp. 188–195, Feb. 2019.

[26] H. Wang, S. Ling, P. X. Liu, and Y.-X. Li, "Control of high-order non-linear systems under error-to-actuator based event-triggered framework," *Int. J. Control*, vol. 95, no. 10, pp. 2758–2770, 2022.

[27] M. Chen, H. Wang, and X. Liu, "Adaptive fuzzy practical fixed-time tracking control of nonlinear systems," *IEEE Trans. Fuzzy Syst.*, vol. 29, no. 3, pp. 664–673, Mar. 2021.

[28] H. Wang, W. Bai, X. Zhao, and P. X. Liu, "Finite-time-prescribed performance-based adaptive fuzzy control for strict-feedback nonlinear systems with dynamic uncertainty and actuator faults," *IEEE Trans. Cybern.*, vol. 52, no. 7, pp. 6959–6971, Jul. 2022.

[29] L. T. Aguilar, Y. Orlov, and L. Acho, "Nonlinear $\mathcal{H}_\infty$-control of nonsmooth time-varying systems with application to friction mechanical manipulators," *Automatica*, vol. 39, pp. 1531–1542, Sep. 2003.

[30] A. Ferrante and L. Ntogramatzidis, "The generalized continuous algebraic Riccati equation and impulse-free continuous-time LQ optimal control," *Automatica*, vol. 50, pp. 1176–1180, Apr. 2014.

[31] T. Ohtsuka, "A recursive elimination method for finite-horizon optimal control problems of discrete-time rational systems," *IEEE Trans. Autom. Control*, vol. 59, no. 11, pp. 3081–3086, Nov. 2014.

[32] A. Laub, "A Schur method for solving algebraic Riccati equations," *IEEE Trans. Autom. Control*, vol. AC-24, no. 6, pp. 913–921, Dec. 1979.

[33] Y. Oshman and I. Bar-Itzhack, "Eigenfactor solution of the matrix Riccati equation–a continuous square root algorithm," *IEEE Trans. Autom. Control*, vol. AC-30, no. 10, pp. 971–978, Oct. 1985.

[34] P. V. Dooren, "A generalized eigenvalue approach for solving Riccati equations," *SIAM J. Sci. Stat. Comput.*, vol. 2, no. 2, pp. 121–135, 1981.

[35] P. Lancaster and L. Rodman, *Algebraic Riccati Equations*. New York, NY, USA: Clarendon Press, 2002.

[36] V. Kučera, "A review of the matrix Riccati equation," *Kybernetika*, vol. 9, no. 1, pp. 42–61, 1973.

[37] R. Buche and H. J. Kushner, "Control of mobile communication systems with time-varying channels via stability methods," *IEEE Trans. Autom. Control*, vol. 49, no. 11, pp. 1954–1962, Nov. 2004.

[38] V. N. Phat and P. Niamsup, "Stability of linear time-varying delay systems and applications to control problems," *J. Comput. Appl. Math.*, vol. 194, pp. 343–356, Oct. 2006.

[39] N. N. Subbotina, "The value functions of singularly perturbed time-optimal control problems in the framework of Lyapunov functions method," *Math. Comput. Model.*, vol. 45, pp. 1284–1293, Jun. 2007.

[40] A. Varga, "Robust pole assignment via Sylvester equation based state feedback parametrization," in *Proc. IEEE Int. Symp. Comput.-Aided Control Syst. Des. (CACSD)*, 2000, pp. 13–18.

[41] X. Le and J. Wang, "Robust pole assignment for synthesizing feedback control systems using recurrent neural networks," *IEEE Trans. Neural Netw. Learn. Syst.*, vol. 25, no. 2, pp. 383–393, Feb. 2014.

[42] S. Li, S. Chen, and B. Liu, "Accelerating a recurrent neural network to finite-time convergence for solving time-varying Sylvester equation by using a sign-bi-power activation function," *Neural Process. Lett.*, vol. 37, no. 2, pp. 189–205, 2013.

[43] Y. Shen, P. Miao, Y. Huang, and Y. Shen, "Finite-time stability and its application for solving time-varying Sylvester equation by recurrent neural network," *Neural Process. Lett.*, vol. 42, no. 3, pp. 763–784, 2015.

[44] H. Huang et al., "Modified Newton integration neural algorithm for dynamic complex-valued matrix pseudoinversion applied to mobile object localization," *IEEE Trans. Ind. Informat.*, vol. 17, no. 4, pp. 2432–2442, Apr. 2021.

[45] A. Noroozi, A. H. Oveis, S. M. Hosseini, and M. A. Sebt, "Improved algebraic solution for source localization from TDOA and FDOA measurements," *IEEE Wireless Commun. Lett.*, vol. 7, no. 3, pp. 352–355, Jun. 2018.

[46] A. G. Dempster and E. Cetin, "Interference localization for satellite navigation systems," *Proc. IEEE*, vol. 104, no. 6, pp. 1318–1326, Jun. 2016.

[47] Y. Zhang, "Towards piecewise-linear primal neural networks for optimization and redundant robotics," in *Proc. IEEE Int. Conf. Netw. Sens. Control*, Apr. 2006, pp. 374–379.

[48] R. H. Sturges, "Analog matrix inversion (robot kinematics)," *IEEE J. Robot. Autom.*, vol. 4, no. 2, pp. 157–162, Apr. 1988.

[49] K. S. Yeung and F. Kumbi, "Symbolic matrix inversion with application to electronic circuits," *IEEE Trans. Circuits Syst.*, vol. 35, no. 2, pp. 235–238, Feb. 1988.

[50] Y. Zhang and J. Wang, "Recurrent neural networks for nonlinear output regulation," *Automatica*, vol. 37, pp. 1161–1173, Aug. 2001.

[51] L. Xiao, Q. Yi, Q. Zuo, and Y. He, "Improved finite-time zeroing neural networks for time-varying complex Sylvester equation solving," *Math. Comput. Simul.*, vol. 178, pp. 246–258, Dec. 2020.

[52] J. Jin, L. Xiao, M. Lu, and J. Li, "Design and analysis of two FTRNN models with application to time-varying Sylvester equation," *IEEE Access*, vol. 7, pp. 58945–58950, 2019.

[53] L. Ding, L. Xiao, K. Zhou, Y. Lan, Y. Zhang, and J. Li, "An improved complex-valued recurrent neural network model for time-varying complex-valued Sylvester equation," *IEEE Access*, vol. 7, pp. 19291–19302, 2019.

[54] S. Li and Y. Li, "Nonlinearly activated neural network for solving time-varying complex Sylvester equation," *IEEE Trans. Cybern.*, vol. 44, no. 8, pp. 1397–1407, Aug. 2014.

[55] L. Xiao, "A finite-time recurrent neural network for solving online time-varying Sylvester matrix equation based on a new evolution formula," *Nonlinear Dyn.*, vol. 90, pp. 1581–1591, Aug. 2017.

[56] Z. Zhang and L. Zheng, "A complex varying-parameter convergent-differential neural-network for solving online time-varying complex Sylvester equation," *IEEE Trans. Cybern.*, vol. 49, no. 10, pp. 3627–3639, Oct. 2019.

[57] C. Yi, Y. Zhang, and D. Guo, "A new type of recurrent neural networks for real-time solution of Lyapunov equation with time-varying coefficient matrices," *Math. Comput. Simul.*, vol. 92, pp. 40–52, Jun. 2013.

[58] X. Lv, L. Xiao, Z. Tan, and Z. Yang, "Wsbp function activated Zhang dynamic with finite-time convergence applied to Lyapunov equation," *Neurocomputing*, vol. 314, pp. 310–315, Nov. 2018.

[59] M. Sun and J. Liu, "A novel noise-tolerant Zhang neural network for time-varying Lyapunov equation," *Adv. Differ. Equ.*, vol. 2020, p. 116, Mar. 2020.

[60] J. Yan, X. Xiao, H. Li, J. Zhang, J. Yan, and M. Liu, "Noise-tolerant zeroing neural network for solving non-stationary Lyapunov equation," *IEEE Access*, vol. 7, pp. 41517–41524, 2019.

[61] L. Xiao, B. Liao, S. Li, Z. Zhang, L. Ding, and L. Jin, "Design and analysis of FTZNN applied to the real-time solution of a nonstationary Lyapunov equation and tracking control of a wheeled mobile manipulator," *IEEE Trans. Ind. Informat.*, vol. 14, no. 1, pp. 98–105, Jan. 2018.

[62] G. Tadmor, "Receding horizon revisited: An easy way to robustly stabilize an LTV system," *Syst. Control Lett.*, vol. 18, no. 4, pp. 285–294, 1992.

[63] W. H. Kwon and S. Han, *Receding Horizon Control* (Advanced Textbooks in Control and Signal Processing). London, U.K.: Springer, 2005.

[64] C. P. Mracek and J. R. Cloutier, "Control designs for the nonlinear benchmark problem via the state-dependent Riccati equation method," *Int. J. Robust Nonlinear Control*, vol. 8, nos. 4–5, pp. 401–433, 1998.

[65] E. B. Erdem and A. G. Alleyne, "Design of a class of nonlinear controllers via state dependent Riccati equations," *IEEE Trans. Control Syst. Technol.*, vol. 12, no. 1, pp. 133–137, Jan. 2004.

[66] J. A. Richards, *Analysis of Periodically Time-Varying Systems* (Communications and Control Engineering), 1st ed. Berlin, Germany: Springer-Verlag, 1983.

[67] B. von de Pol, "Forced oscillations in a circuit with non-linear resistance (receptance with reactive triode)," *London Edingburg Dublin Phil. Mag.*, vol. 3, pp. 65–80, Jan. 1927.

[68] H. Wang, K. Xu, P. X. Liu, and J. Qiao, "Adaptive fuzzy fast finite-time dynamic surface tracking control for nonlinear systems," *IEEE Trans. Circuits Syst. I, Reg. Papers*, vol. 68, no. 10, pp. 4337–4348, Oct. 2021.

[69] V. N. Katsikis, P. S. Stanimirović, S. D. Mourtas, L. Xiao, D. Stanujkić, and D. Karabašević, "Zeroing neural network based on neutrosophic logic for calculating minimal-norm least-squares solutions to time-varying linear systems," *Neural Process. Lett.*, to be published.

Theodore E. Simos was born in Athens, Greece, in 1962. He received the Ph.D. degree in numerical analysis from the Department of Mathematics, National Technical University of Athens, Athens, in 1990.

He is a Professor and a Leading Scientist with the Laboratory of Inter-Disciplinary Problems of Energy Production, Ulyanovsk State Technical University, Ulyanovsk, Russia, a Research Fellow with the Center for Applied Mathematics and Bioinformatics, Gulf University for Science and Technology, Mubarak Al-Abdullah, Kuwait, a Research Fellow with the Department of Medical Research, China Medical University Hospital, China Medical University, Taichung City, Taiwan, a Distinguished Professor with the Data Recovery Key Laboratory of Sichun Province, Neijiang Normal University, Neijiang, China, and a Visiting Professor with the Democritus University of Thrace, Xanthi, Greece. He has many collaborations with several Universities all over the world. He is the Founder and the Chairman of two international conferences. He is the author of over 650 peer-reviewed publications and he has more than 6000 citations (excluding self-citations). His research interests are on numerical analysis and specifically on: numerical solutions of differential equations, scientific computing, and optimization.

Prof. Simos was a Highly Cited Researcher in Mathematics (Lists 2001–2013, 2017, and 2018). He is the editor-in-chief of three scientific journals and an editor of more than 30 scientific journals. He is a reviewer in several other scientific journals and conferences. He is an Active Member of the European Academy of Sciences and Arts and the European Academy of Sciences, and a Corresponding Member of the European Academy of Sciences, Arts and Letters.

Vasilios N. Katsikis received the B.S. degree in mathematics from the National and Kapodistrian University of Athens, Athens, Greece, in 1997, and the M.Sc. degree in applied mathematics and the Ph.D. degree in mathematics from the National Technical University of Athens, Athens, in 2000 and 2006, respectively.

He is currently an Associate Professor of Mathematics and Informatics and the Director of the Division of Mathematics–Informatics and Statistics–Econometrics, Department of Economics, National and Kapodistrian University of Athens. Throughout his research career, he has over 130 publications in various peer-reviewed scientific journals. His main research interests include neural networks, matrix analysis, linear algebra, and intelligent optimization.

Spyridon D. Mourtas received the B.S. degree in mathematics from the University of Patras, Patras, Greece, in 2016, and the M.Sc. degree in applied economics and finance and the Ph.D. degree in economics from the National and Kapodistrian University of Athens, Athens, Greece, in 2019 and 2023, respectively.

His main research interests include neural networks, matrix analysis, and intelligent financial optimization.

Predrag S. Stanimirović received the Ph.D. degree in mathematics from the Faculty of Philosophy, University of Niš, Niš, Serbia, in 1996.

He is currently working as a Full Professor with the Faculty of Sciences and Mathematics, Department of Computer Science, University of Niš and with the Laboratory "Hybrid Methods of Modelling and Optimization in Complex Systems," Siberian Federal University, Krasnoyarsk, Russia. His interest in research encompasses diverse fields of mathematics, applied mathematics, and computer science, which span multiple branches of numerical linear algebra, recurrent neural networks, symbolic computation, and operations research. Throughout his research career, he has published over 350 publications in various scientific journals, including six research monographs.

Prof. Stanimirović is an Editor in scientific journals, such as *Filomat*, *Electronic Research Archive*, *Journal of Mathematics*, and *Facta Universitatis, Series: Mathematics and Informatics* and several other journals.